AD-A087 998 SRI INTERNATIONAL MENLO PARK CA F/G 18/3
MISERS BLUFF ELECTROMAGNETIC PROPAGATION EXPERIMENTS. VOLUME II--ETC(U)
OCT 79 A A BURNS DNA001-77-C-0269
UNCLASSIFIED DNA-4806T-3 NL

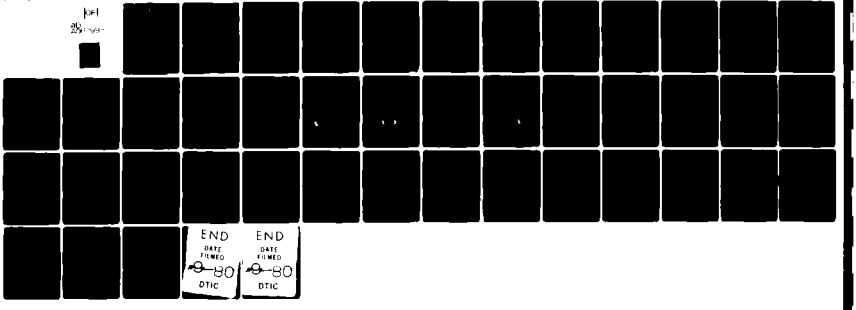

END DATE FILMED 9-80 DTIC

END DATE FILMED 9-80 DTIC

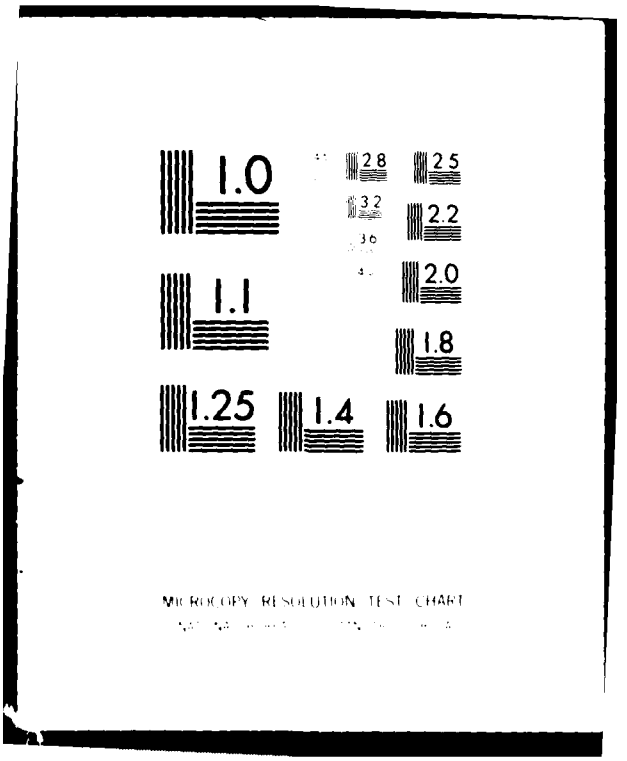
1.0
2.8
2.5
3.2
2.2
3.6
2.0
1.1
1.8
1.25
1.4
1.6
MICROCOPY RESOLUTION TEST CHART

LEVEL II

DNA 4806T-3

MISERS BLUFF ELECTROMAGNETIC PROPAGATION EXPERIMENTS

Volume III – Preliminary Results of the UHF-EHF Radar-Scattering and Coherent-Transmission Experiments

Alan A. Burns
SRI International
333 Ravenswood Avenue
Menlo Park, California 94025

1 October 1979

Topical Report for Period 1 October 1978—31 March 1979

CONTRACT Nos. DN DNA 001-77-C-0269 AND
DN DNA 001-79-C-0181

APPROVED FOR PUBLIC RELEASE;
DISTRIBUTION UNLIMITED.

THIS WORK SPONSORED BY THE DEFENSE NUCLEAR AGENCY UNDER RDT&E RMSS CODES B322077462 I25AAXHX68501 H2590D, B322078462 I25AAXHX68502 H2590D AND B322079462 I25AAXHX68503 H2590D.

Prepared for
Director
DEFENSE NUCLEAR AGENCY
Washington, D. C. 20305

63-4104

Destroy this report when it is no longer needed. Do not return to sender.

PLEASE NOTIFY THE DEFENSE NUCLEAR AGENCY, ATTN: TISI, WASHINGTON, D.C. 20305, IF YOUR ADDRESS IS INCORRECT, IF YOU WISH TO BE DELETED FROM THE DISTRIBUTION LIST, OR IF THE ADDRESSEE IS NO LONGER EMPLOYED BY YOUR ORGANIZATION.

(18) DNA, SBIE

UNCLASSIFIED

SECURITY CLASSIFICATION OF THIS PAGE (When Data Entered)

(19) **REPORT DOCUMENTATION PAGE**

READ INSTRUCTIONS BEFORE COMPLETING FORM

1. REPORT NUMBER DNA 4806T-3	2. GOVT ACCESSION NO. AD-A087 998
4. TITLE (and Subtitle) MISERS BLUFF ELECTROMAGNETIC PROPAGATION EXPERIMENTS. Volume III—Preliminary Results of the UHF-EHF Radar-Scattering and Coherent-Transmission Experiments.	5. TYPE OF REPORT & PERIOD COVERED Topical Report, for Period 1 Oct 78—31 Mar 79
	6. PERFORMING ORG. REPORT NUMBER SRI Projects 6462 and 8279
7. AUTHOR(s) Alan A. Burns	8. CONTRACT OR GRANT NUMBER(s) DNA 001-77-C-0269, DNA 001-79-C-0181
9. PERFORMING ORGANIZATION NAME AND ADDRESS SRI International 333 Ravenswood Avenue Menlo Park, California 94025	10. PROGRAM ELEMENT, PROJECT, TASK AREA & WORK UNIT NUMBERS Subtasks I25AAXHX685-01, -02 and -03
11. CONTROLLING OFFICE NAME AND ADDRESS Director Defense Nuclear Agency Washington, D.C. 20305	12. REPORT DATE 1 October 1979 13. NUMBER OF PAGES 42
14. MONITORING AGENCY NAME & ADDRESS (if different from Controlling Office) (12) 41	15. SECURITY CLASS (of this report) UNCLASSIFIED 15a. DECLASSIFICATION DOWNGRADING SCHEDULE

16. DISTRIBUTION STATEMENT (of this Report)

Approved for public release; distribution unlimited.

17. DISTRIBUTION STATEMENT (of the abstract entered in Block 20, if different from Report)

18. SUPPLEMENTARY NOTES

This work sponsored by the Defense Nuclear Agency under RDT&E RMSS Codes B322077462 I25AAXHX68501 H2590D, B322078462 I25AAXHX68502 H2590D and B322079462 I25AAXHX68503 H2590D.

19. KEY WORDS (Continue on reverse side if necessary and identify by block number)

MISERS BLUFF
Nuclear Weapons Effects
Dust Effects
Electromagnetic Propagation
Millimeter Waves

20. ABSTRACT (Continue on reverse side if necessary and identify by block number)

SRI International fielded four electromagnetic propagation experiments during the MISERS BLUFF II high explosive tests. Two of the four experiments are discussed here, selected preliminary results are presented, and some tentative conclusions drawn. The UHF-EHF Coherent-Transmission Experiment measured the amplitude and phase changes suffered by a number of phase-coherent CW signals transmitted through a volume of space above ground zero. The signals experienced phase retardations and absorption due to the mass of soil injected into

DD FORM 1 JAN 73 1473 EDITION OF 1 NOV 65 IS OBSOLETE

UNCLASSIFIED

SECURITY CLASSIFICATION OF THIS PAGE (When Data Entered)

419 211

20. ABSTRACT (Continued)

the signal paths, and further extinction due to scattering loss from the dust particles. Diffractive and refractive propagation effects also occurred. The SHF/EHF-Scattering Experiment used a four-frequency radar system to measure backscatter from and transmission losses through the dust clouds in the 10-GHz to 100-GHz range. Radar effects of dust clouds were measured, and data were collected from which dust densities and particle-size distributions can be inferred. A great deal of internal structure was evident in the MBII-2 dust cloud.

PREFACE

The material comprising this topical report is virtually the same as that to be published in the proceedings of the MISERS BLUFF Data-Review Meeting, held in Albuquerque, NM,, in March 1979. Because of the interest in our measurements, we have decided to publish these preliminary results as a separate entity.

Under the direction of Mr. E. E. Martin, the Georgia Institute of Technology Engineering Experiment Station provided the radars and operated them for the SHF/EHF-Scattering Experiment. They have also done the quick-look data reduction. Many of their results have been incorporated into this report.

The SHF/EHF-scattering experiment was jointly sponsored by the Defense Nuclear Agency, the U.S. Army Ballistic Missile Defense Advanced Technology Center, and the U.S. Army Ballistic Missile Defense Systems Command.

CONTENTS

ILLUSTRATIONS

TABLES

I INTRODUCTION

Under the sponsorship of the Defense Nuclear Agency, the U.S. Army Ballistic Missile Defense Advanced Technology Center and Systems Command, and the U.S. Air Force Space and Missile Systems Organization, SRI International fielded a series of electromagnetic propagation experiments during the MISERS BLUFF II high explosive (HE) tests. These experiments were carefully designed to accurately measure the effects of the large dust clouds lofted by the detonations on signals ranging in wavelength from 100 m (3 MHz) to 0.53 μm (green light). All of the experiments were intended to collect data that would be useful for nuclear-code validation and for direct extrapolation into the nuclear environment. We will discuss two of the four experiments: the UHF-EHF Coherent-Transmission Experiment, and the SHF/EHF-Scattering (radar) Experiment. The laser and MF experiments are described elsewhere.[1,2]*

Both MISERS BLUFF II tests took place at the Planet Ranch test site on the dry bed of the Bill Williams River near Lake Havasu City, Arizona. The first test, MISERS BLUFF II-1 (MBII-1), which was a 120-ton ammonium nitrate and fuel oil (ANFO) detonation, took place at 1300 MST on 28 June 1978. The second test, MBII-2, consisted of the simultaneous detonation of six such 120-ton ANFO charges uniformly spaced on the periphery of a 100-m-radius circle. This test took place at 1100 MST on 30 August 1978. Although the primary objective of the MBII tests was the study of ground motions in a multiple-burst environment in support of the MX program, these tests provided a good opportunity to measure dust effects as well. Our experiments were added and were conducted on a noninterference basis.

However, as we have pointed out before, in connection with the DICE THROW tests,[3,4] the capped-cylinder ANFO charge configuration does not

*All references are listed at the end of the report.

lead to a good simulation of the nuclear environment. Hydrodynamic-code calculations, which are consistent with observations,[4] predict a "reverse" vortex at the beginning, with a downward flow in the center of the dust cloud. This effect and the rather low flow-field velocities in general lead to rapid fallout, particularly of the larger particles. Because the large particles dominate the dust-cloud effects,[4] the enhanced fallout of the large particles leads to an early cessation of strong effects. Thus, direct extrapolation from the single-capped cylinder ANFO configuration to the nuclear environment can lead to an underestimation of dust effects and, particularly, of their duration. Since very little is known about the flow fields of the multiple-charge MBII-2 test, extrapolation may be even more risky. Nevertheless, these experiments have provided the best data, so far, concerning the effects of large, high-density dust clouds on electromagnetic propagation.

Although all four experiments are interrelated, the two on which we will focus were related most closely, in that they used very nearly the same part of the electromagnetic spectrum. Thus, the interactions of the radio-wave energy with the matter in the clouds were similar or different aspects of the same phenomenon. For example, the transmission and absorption effects result from the bulk forward-scattering effects of many particles; scattering loss and backscatter strength are also closely related. These two experiments, therefore, measured different aspects of the same underlying phenomenon and together can provide greater understanding than the sum of each done separately. Although the analysis of the data has only recently begun, preliminary results do show a high degree of consistence between the two experiments.

Figure 1 is a map showing the locations of the various components of these experiments in relation to ground zeros. The two transmitters for the transmission experiment were located on a ridge about 1 km south of ground zero. Because the line of sight to the receiver had to pass above ground zero, for MBII-2 the receiver was moved nearly 3 km east of its MBII-1 location. A "phase-repeater" station, placed at the Planet Ranch gate on the road north, provided a means for relaying a reference signal from the transmitter to the receiver along a path unaffected by

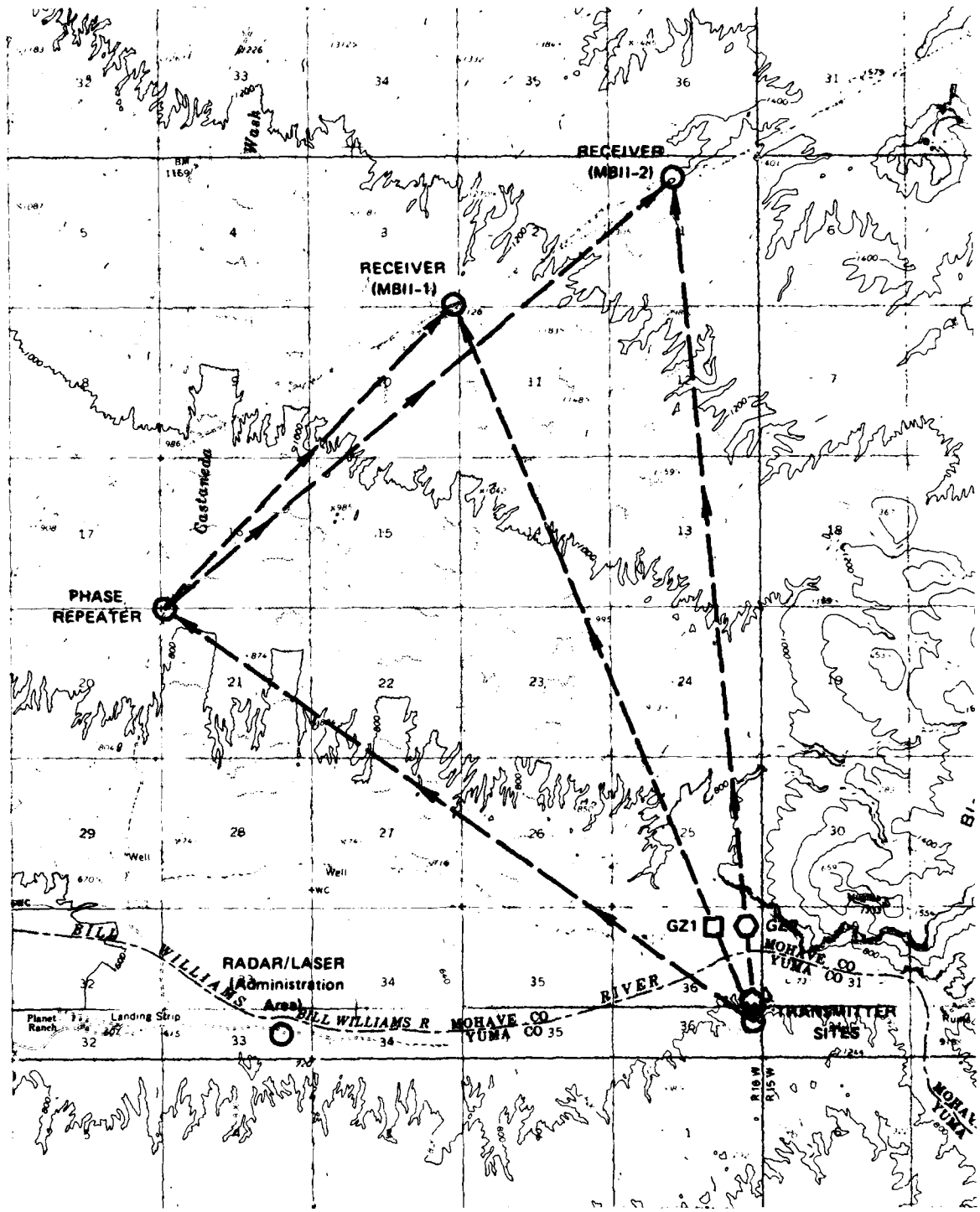

FIGURE 1 POSITIONS OF MISERS BLUFF UHF-EHF EM PROPAGATION EXPERIMENT ELEMENTS

the detonations. Unfortunately, the best place to put the radar system (and the laser system, too) turned out to be the same location chosen for the administration area. It was necessary to overcome problems caused by dust raised by traffic and by electromagnetic interference from nearby communications transmitters. The difficult terrain precluded finding a better location. We also fielded extensive photographic coverage (primarily in the form of boresight cameras) in support of these experiments.

II THE UHF-EHF-COHERENT-TRANSMISSION EXPERIMENT

The UHF-EHF-Coherent-Transmission Experiment measured amplitude and phase changes produced by the dust clouds. When all the dust particles are much smaller in circumference than the radio wavelength, theory predicts that the phase shifts and the absorption component of extinction of the electromagnetic energy are independent of the particle-size distribution. Hence, the observed phase shift is proportional to the integrated dust density through the cloud, if distortions from propagation effects such as diffraction are not serious. On the other hand, the scattering-loss contribution to extinction is very sensitive to the particle-size distribution. Without some independent information, such as the amount of absorption per unit phase shift or the amount of scattering, the two extinction components cannot be separated.

For the MISERS BLUFF data, we have three ways to estimate the relative contributions of scattering loss and absorption to attenuation. First, soil samples were collected and are presently being tested in the laboratory to determine their ratios of absorption to phase shift. Second, the wavelength dependence of attenuation is used to estimate the relative contributions of absorption and scattering loss. Finally, the SHF/EHF-Scattering Experiment measures backscattering directly, from which total scattering is estimated. Because none is perfect, three methods will be used to gain a consistent explanation.

The third method was not available for a very similar set of measurements made during the DICE THROW Main Event.[3] These MISERS BLUFF measurements used essentially the same equipment (various modifications were made) as that for DICE THROW. The main differences were (1) the addition of millimeter-wavelength capability, (2) the size of the antennas, and (3) the locations of receivers and transmitters in relation to the ground zeros.

For MISERS BLUFF, the main transmitter was placed as high as practicable on a ridge to the south of the ground zeros and was not moved after MBII-1. The secondary transmitter was placed as low as possible on the ridge while providing a line of sight to the receiver. It was necessary to relocate the secondary transmitter after MBII-1 in order to put it on the same radial as the main transmitter from the MBII-2 ground zero. The receiver used a central antenna structure and two outriggers located about 100 m roughly east and west of the central structure. A van near the central structure housed most of the receiving equipment and the data-acquisition and recording system.

The combination of two transmitters and three receiving locations provided six transmission paths through a volume in the range between about 70 m and 110 m above the ground zeros. The azimuthally-spread paths passed 15 m east and west of the central signal path in the vicinity of ground zero. Table 1 lists the various signals transmitted along those lines of sight and their characteristics. The largest number of the signals were transmitted between the main transmitter and the main receiver along paths passing directly above the ground zeros. All the signals were coherent with one another; both amplitude and phase changes could be measured accurately.

Both digital and analog data-recording methods were used. The primary data-acquisition system was digital, whereby the quadrature components of each of the signals were detected in a 150-Hz bandwidth and digitized at 500 Hz. Redundant digital tape recorders were used to reduce the effect of any malfunction. In addition, as a backup, the 50-kHz IF signals were recorded using an analog machine. Some problems with the digitizing system were encountered on both events. In both cases the problems resulted in the insertion of extraneous symbols into the digital data stream. However, the offending quantities were easily identified and have been deleted automatically with no loss of data.

One of our major goals was to extend these measurements, which were first made on the DICE THROW main event, to the millimeter-wave regime. Thus, a 35-GHz and a 95-GHz link were added for MISERS BLUFF II.

Table 1

UHF-EHF-COHERENT-TRANSMISSION EXPERIMENT LINKS

Identifier	Path*	Band	Frequency (MHz)
O-UR	MT-PR	UHF	413
O-LR	PR-MR	L	1,239
1-S	MT-MR	S	2,891
2-XR	ST-MR	X	10,188
3-X	MT-MR	X	8,915
4-W	MT-MR	W	95,937
5-UR	ST-EO, MR,WO†	UHF	424
6-UC	MT-MR	UHF	413
7-K	MT-MR	K_a	33,536
8-L	MT-MR	L	1,274
9-U2	MT-EO	UHF	413
10-X2	MT-EO	X	8,915
11-U3	MT-WO	UHF	413
12-X3	MT-WO	X	8,915

*MT = Main transmitter
ST = Secondary transmitter
MR = Main receiver
EO = East outrigger
WO = West outrigger
PR = Phase repeater.

†Time-multiplexed.

State-of-the-art devices were required for those links, however, and they proved to be unreliable in the field environment. (The 35-GHZ devices were returned several times to the manufacturer for reworking, and the 95-GHz units were delivered several months late, only a few days before MBII.)* As a result, no millimeter-wavelength dust-cloud effects

*During MBII-1, the 35-GHz transmitter lost internal phase-lock during shock-wave passage shortly after detonation.

data were collected; turbulence effects at 35 GHz were seen behind the shockwave on MBII-1. Although the rest of this experiment was very successful, the loss of data in this very interesting wavelength range was very disappointing.

In-depth data analysis has just begun and only preliminary results are available now. Figures 2(a) and (b) show the raw 8.9-GHz Path-2 amplitude and phase results for MBII-1 and -2. The much stronger effects during MBII-2 result from the much greater mass of material lofted by the larger detonation (the MBII-1 crater-volume estimate was 1600 m^3, while the sum of the MBII-2 crater-volumes was 10,200 m^3.* Although the phase shifts are proportional for nearly all conditions to the integrated dust-mass density along the signal paths, the phase data shown in Figure 2 cannot be interpreted properly in terms of average dust density until they are compared to the photographic records. It is reasonable, however, that the MBII-2 phase fluctuations are about twice those from MBII-1 [note the scale change between Figures 2(a) and 2(b)].

Figure 3 shows the amplitude fluctuations measured on the upper azimuthally separated signal paths at 8.9 GHz, which may be further compared with the central path data of Figure 2(b). There is a progression from least to most severe effects as the paths shift toward the west, which produced about 10 dB of general attenuation along with the severe fading seen on all three paths. Because these paths were only laterally separated by about 15 m above ground zero, there was obviously a great deal of inhomogeneity over short distances within the dust cloud at these early times.

Signal perturbations measured during the MISERS BLUFF II tests were considerably weaker than those seen during DICE THROW.[3] Part of the difference can be attributed to the higher-altitude signal paths above ground zero on the later events. The smallness of the MBII-1 charge also contributed to this difference. One important effect seen during DICE THROW did not occur during MISERS BLUFF; i.e., the complete loss of the coherent

*Data furnished by Capt. R. J. Davis, FCDNA.

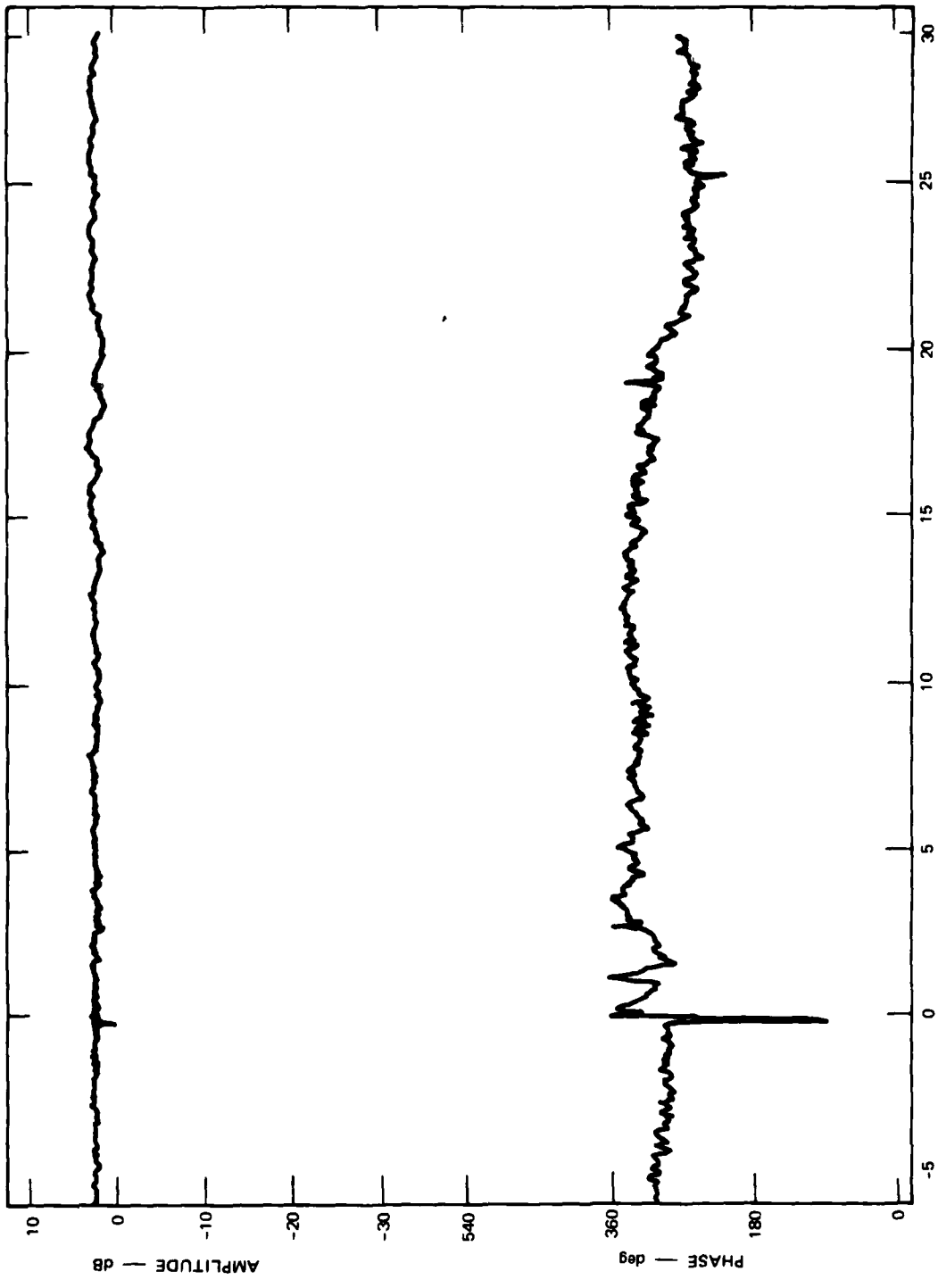

FIGURE 2(a) MBII-1 UHF-EHF TRANSMISSION EXPERIMENT, PATH 2--8.9-GHz AMPLITUDE AND PHASE RESULTS

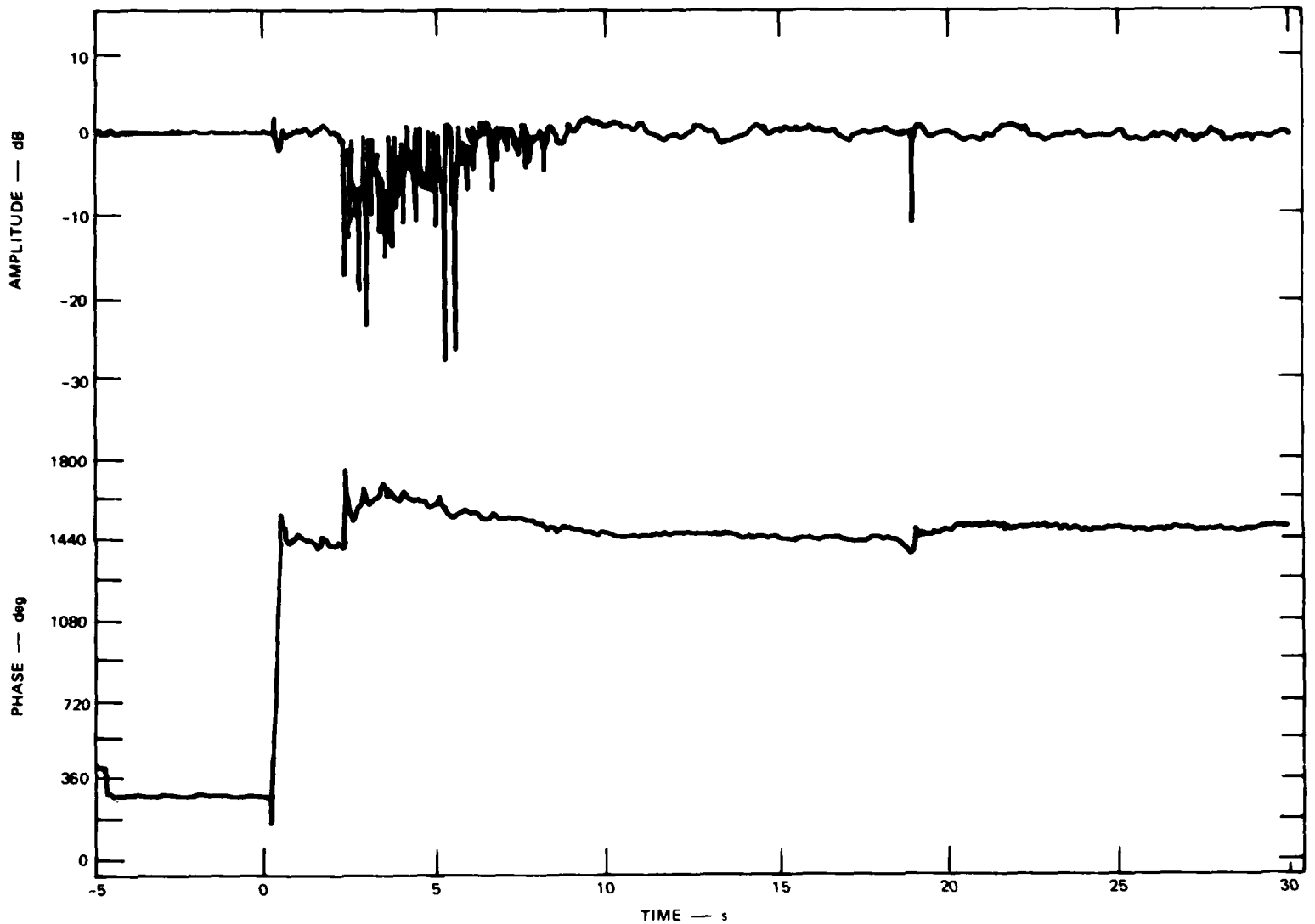

FIGURE 2(b) MBII-2 UHF-EHF TRANSMISSION EXPERIMENT, PATH 2--8.9-GHz AMPLITUDE AND PHASE RESULTS

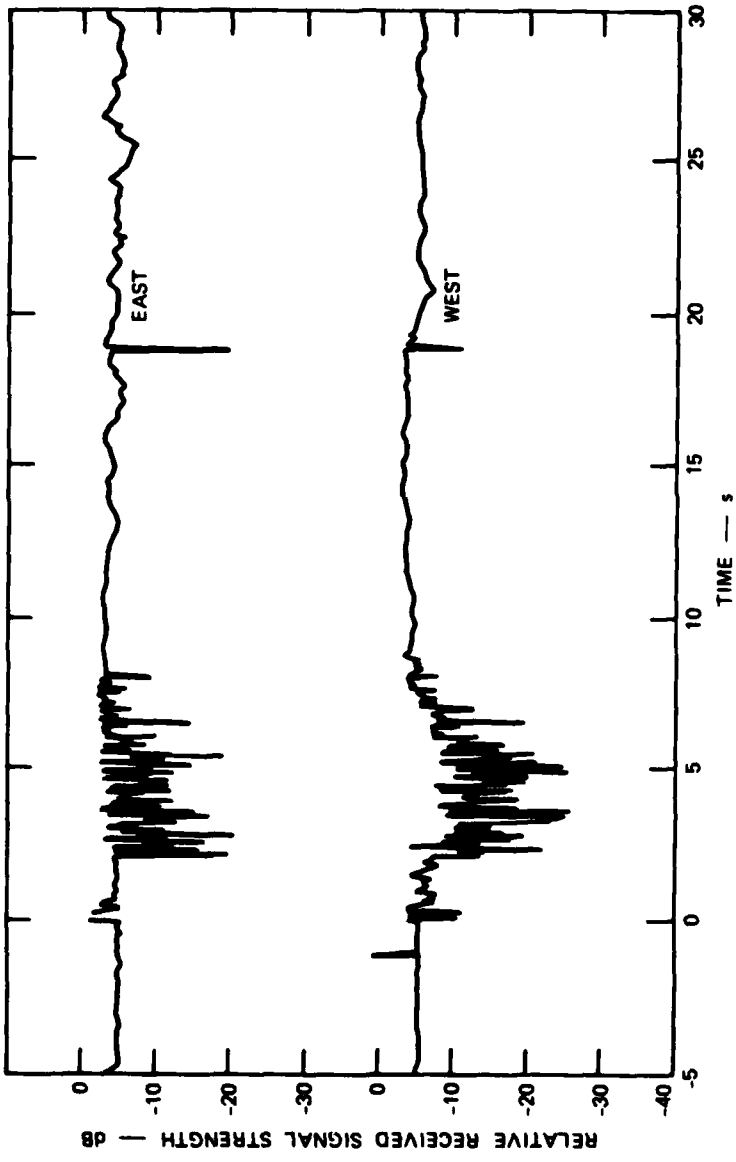

FIGURE 3 MBII-2 UHF-EHF TRANSMISSION EXPERIMENT--8.9-GHz AMPLITUDE FLUCTUATIONS FROM AZIMUTHALLY SEPARATED SIGNAL PATHS

signal accompanied by strong attenuation and apparent saturation of maximum attenuation. This has been interpreted as caused by the sudden transition to a multiple-scattering condition when many large particles were present. Apparently, that condition was not encountered during MISERS BLUFF, possibly because of a scarcity of large particles.

Figure 4 is a comparison of the amplitude effects observed at different wavelengths on the main signal path. As expected, the fluctuations were more severe at the shorter wavelengths. Although the duration of the most severe effects covered almost the same time intervals, both the amplitude and phase fluctuations measured during MBII-2 were weaker than those seen during the DICE THROW Main Event, in spite of the much larger crater volume and presumably greater mass of material lofted for the later event. (The sum of the MBII-2 apparent crater volumes* was 1.0×10^4 m^3 versus 4.6×10^3 m^3 for the DICE THROW Main Event crater.) Most of the difference is probably due to the altitude difference of the signal paths above ground zero (about 6 m for DT compared to 100 m for MBII-2). Other factors leading to important differences may be variations in the particle-size distributions and the electromagnetic properties of the soil. (We are currently measuring those properties of several MB soil samples collected from the ground-zero area before and after the events.) The amount of moisture present also has a strong effect on the amount of absorption by a dust cloud.

The first steps in the data-processing and interpretation effort currently under way are to calibrate the data carefully and to remove the artifacts that can be seen at various times in Figures 2, 3, and 4, particularly in the phase data (the perturbations at about T + 19 s were caused by the shock wave hitting the receiving system). The next steps are to compare and correlate the results with other data and information, including photographic, radar, and optical data, and the results of the

*Data furnished by Capt. R. J. Davis, FCDNA.

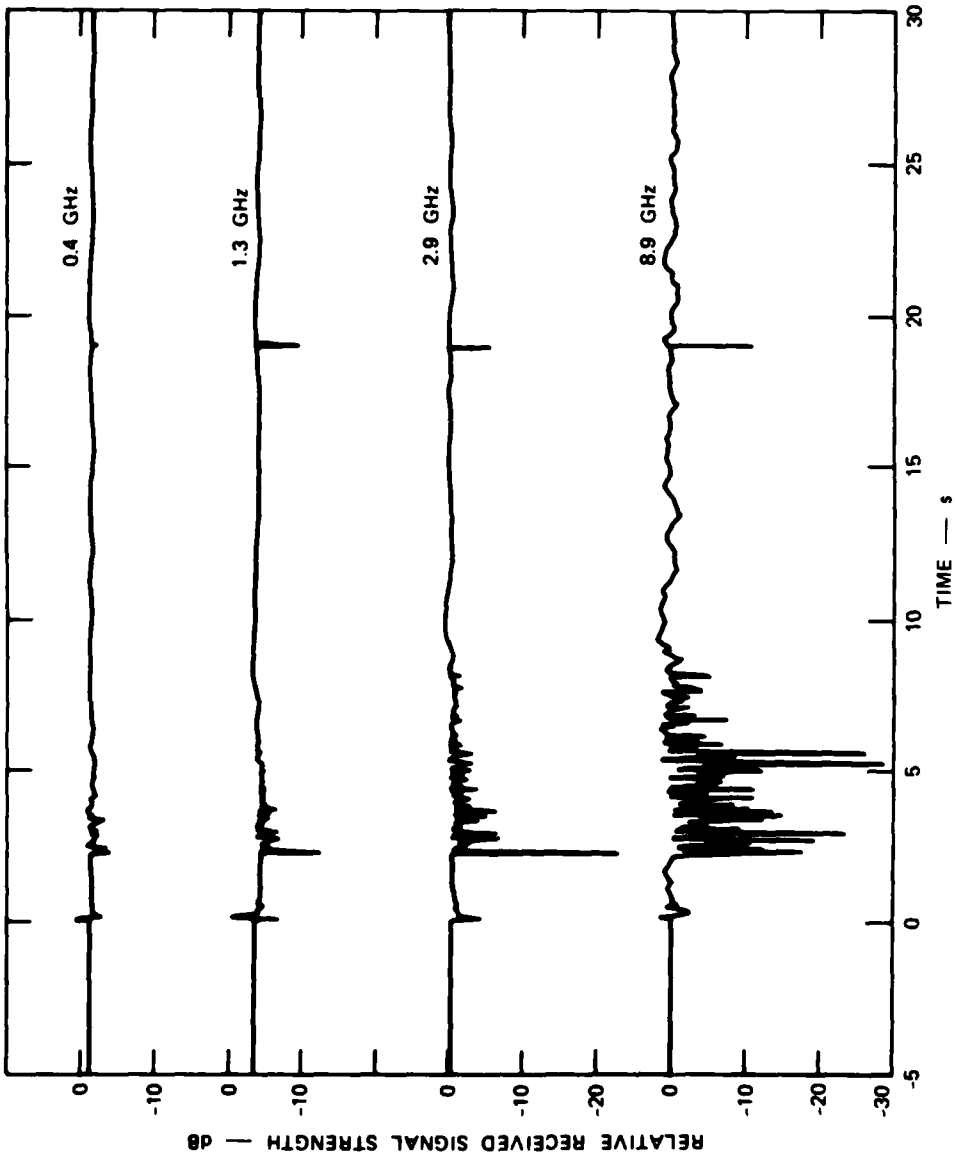

FIGURE 4 MBII-2 UHF-EHF TRANSMISSION EXPERIMENT--MAIN SIGNAL PATH AMPLITUDE FLUCTUATIONS

soil sample electromagnetic properties measurements.* Including the results from DICE THROW Main Event, we now believe that we have sufficient experimental measurements to characterize the problem of propagation through dust clouds in the 0.4-GHz-to-10-GHz range. By extending the soil sample measurements to millimeter wavelengths, we expect to gain enough knowledge to make reasonable extrapolations beyong 10 GHz possible, even though we have very little direct experimental data in that range.

*The first results from the electromagnetic properties measurements indicate that this soil was particularly lossy. Loss tangents as high as 0.14 have been measured in the 1-GHz to 18-GHz interval.

III SHF/EHF-SCATTERING EXPERIMENT

In contrast to those of UHF-EHF-Coherent-Transmission Experiment, SHF/EHF-Scattering Experiment measurements were expected to be very sensitive to the particle-size distribution. Indeed, one of our main goals was to measure the dependence of the particle-size distribution function of time and position. The other principal objectives were the measurements of the effects of large-scale explosively-produced dust clouds on millimeter radar systems and measurements of the mass density in the clouds. These data are valuable for extrapolation into the much more severe nuclear environment and for verifying methods to predict effects in the nuclear environment.

Physically, this experiment consisted of a four-frequency radar system and a data-acquisition and control system. Table 2 lists the parameters of the radar system, which was provided, installed, and operated by the Engineering Experiment Station of the Georgia Institute of Technology under a subcontract to SRI International. Unfortunately, the 95-GHz radar was at least 20 dB less sensitive than was planned, primarily because of low power output and the need for a wide-bandwidth IF system. The 70-GHz radar was included principally as a backup. The four antennas were scaled in size to provide nearly equal beamwidths and were mounted on the same pedestal. Because all four radars used the same pulse width and the antennas were boresighted together, nearly the same volume in the dust cloud provided the echoes. Although this approach carried a penalty of reduced sensitivity at the shorter wavelengths, it removed uncertainties that would have resulted from dissimilar scattering volumes.

A minicomputer/microprocessor system constructed by SRI International controlled the pedestal and did the real-time digitization of the echoes. This system was very flexible, and changes in antenna scan-pattern parameters and range-gate positions and sizes could be made very rapidly.

Table 2

MBII-2 RADAR PARAMETERS

Parameter	Radar			
	1	2	3	4
Frequency (GHz)	9.375	35	69.7	94.5
Antenna				
Size (ft)	10	3	1.5	
Beamwidth E plane	0.78°	0.70°	0.70°	0.70°
Beamwidth H plane	0.70°	0.62°	0.65°	0.66°
Isolation H/V (dB)	40	40	40	40
Gain (dB)	47	48	48	46
Polarization	Dual H/V	Dual H/V	Dual H/V	Dual H/V
Transmitter	Magnetron	Magnetron	Magnetron	EIO
Type	2J42	M5123	BL246	VITB 2443
Power output (kW)	6.2	5.9	0.8	0.8
Pulse width (ns)	250	250	250	250
PRF (Hz)	1000	1000	1000	1000
Receiver				
Mixer	Balanced	Balanced	Single	Single
MDS (dBm)	-93	-90	-63	<-59
Bandwidth (MHz)	12	12	80	80
Dynamic range (dB)	70	70	50	70
Detection	Log	Log	Log	Log

Two independent range gates were provided. The first gate was used on cloud echoes, while the second gate was set at the range of a corner reflector placed on top of the mesa behind ground zero. Another corner reflector was placed lower on the mesa within the span of the first range gate. Echoes from the reflectors and from the mesa itself allowed measurements of two-way extinction through the clouds. The values of observed extinction will be compared with the transmission-experiment results and will be used for compensation for the attenuation of echoes from regions of the clouds most distant from the radar.

In this brief report we will concentrate on the MBII-2 measurements. Figure 5 shows the pre-event 9.3-GHz and 35-GHz radar echoes (only the expected, horizontally polarized echoes will be presented here).* Before T - 0, the radar beams were pointed just above ground zero. Echoes from a low peninsula jutting into the river bed extend from 4.2 km to 4.4 km and those from the mesa beyond ground zero start at 5.2 km; the second range gate extended from 6.0 km to 6.3 km. Neither corner reflector was in the beams at that time.

The radar beams were not moved until about T + 7 s (there was a small amount of jitter due to wind loading). Figure 6 shows the 9.3-GHz and 35-GHz echoes at T + 4 s, which filled the space from 4.6 km to 5.2 km, where the mesa echoes began. Also shown are the pre-event peak echo strength from the mesa. While the 9.3-GHz echoes are practically unchanged the 35-GHz echoes appear to have been attenuated by about 10 dB (two-way).

By T + 8 s (Figure 7), the cloud echoes had a very pronounced structure, which is undoubtedly because of the manner in which the six-charge MBII-2 array was viewed (in pairs) from the radar. It is noteworthy that a two-orders-of-magnitude change in the 35-GHz echo strength (and, roughly, of dust density) occurred between adjacent 37.5-m range cells. Note also that the echo strength has decreased significantly.

---

*Data reduction is being done by the Georgia Institute of Technology under an SRI subcontract.

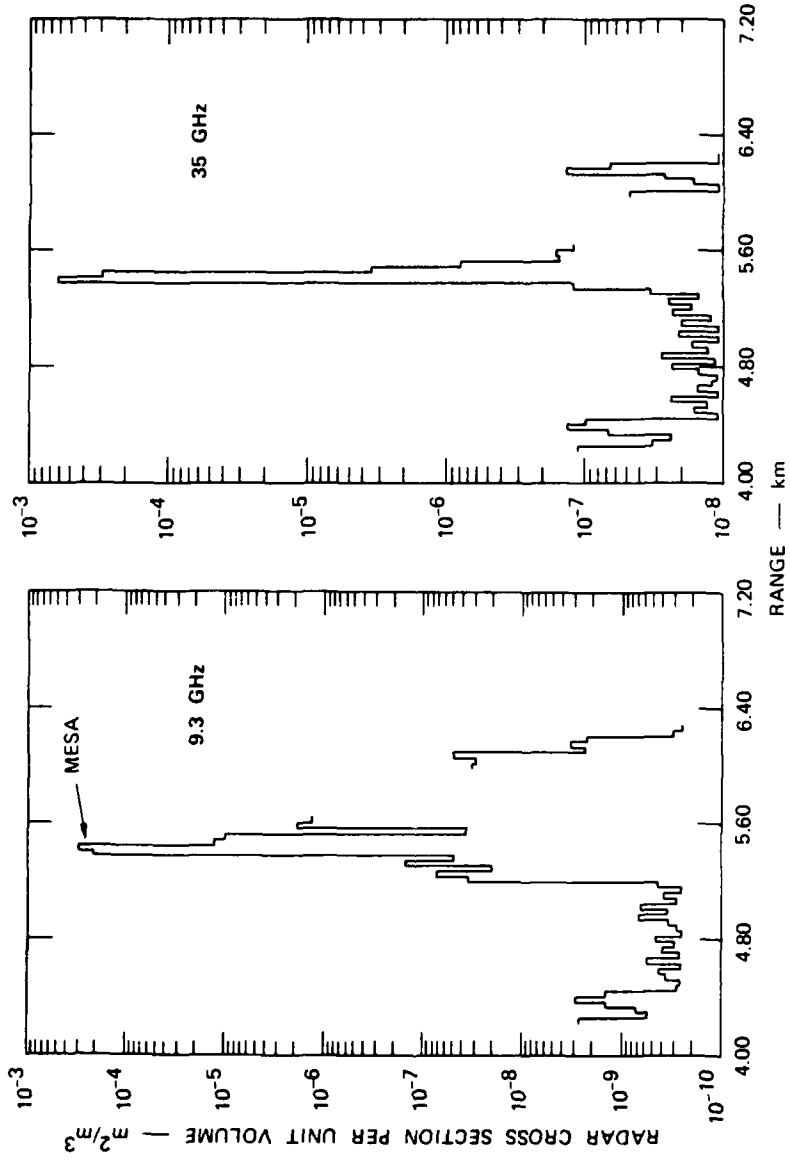

FIGURE 5 MBII-2 RADAR ECHOES AT 9.3 AND 35 GHz AT T-10 s--AZIMUTH = 73.8°, ELEVATION = 0.4°

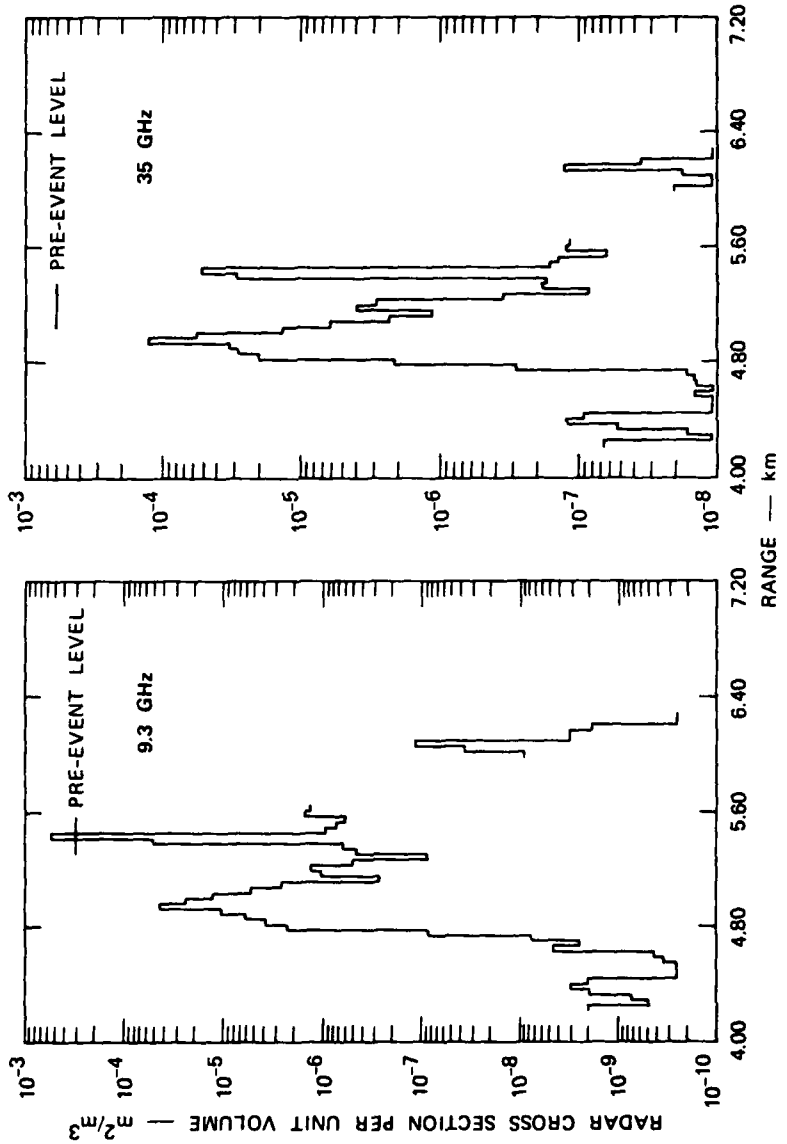

FIGURE 6 MBII-2 RADAR ECHOES AT 9.3 AND 35 GHz AT T + 4 s--AZIMUTH = 73.6°, ELEVATION = 0.4°

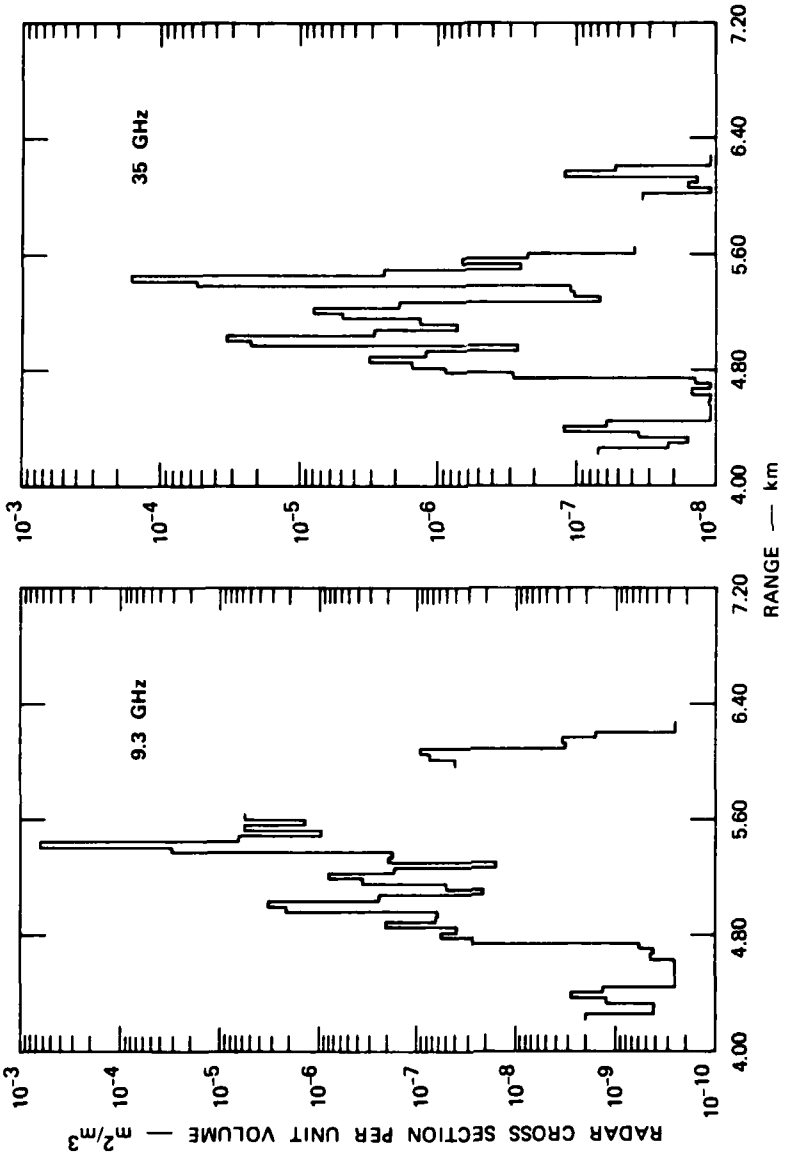

FIGURE 7 MBII-2 RADAR ECHOES AT 9.3 AND 35 GHz AT T + 8 s--AZIMUTH = 73.4°, ELEVATION = 0.6°

At T + 8 s, the radar beam was being moved from its original position to that required to illuminate the lower corner reflector. Although it was thought to have been well-anchored, the lower corner reflector was knocked over by the explosion. The cloud echoes had a structure similar to those at T + 8 s, although their strengths had decreased further. At T + 13 s, the beams were moved higher to illuminate the upper corner reflector because it had been occulted by the cloud. The triple structure of the echoes was still present at T + 16 s (Figure 8) with very abrupt changes in short distances, which indicates that little or no mixing had occurred.

By T + 42 s, however, it appears that most of the structure had dissipated, at least at the base of the cloud cap. Figure 9 shows the 9.3-GHz and 35-GHz echoes at that time, which corresponds to the bottom of one of the automatic vertical raster scans that were initiated at about T + 30 s. Similar echoes, with little structure, were seen at T + 40 s and T + 44 s, when the beams were directed at slightly higher parts of the dust cloud. However, at T + 94 s, when the radar was pointed high in the cloud, there was a great deal of structure.

Figure 10 summarizes the first 94 s of 9.3-GHz and 35-GHz expected polarization sense echoes. There was an initial rapid decrease in echo strength (and dust density) that lasted until about T + 15 s, followed by a slower decline. The initial decrease corresponds to the period of rapid fallout of most of the material lofted by the explosion. No corrections have been made for effects such as extinction and beam motion, however, so these results should be considered to be very preliminary.

We believed at first that no detectable echoes were obtained at 95 GHz. However, subsequent analysis revealed the definite presence of echoes at ranges corresponding to those giving maximum return at the longer wavelengths at early times. Figure 11 shows an example. Although statistical tests of significance need to be made, we believe that echoes can be seen as late as T + 8 s.

To aid in the planning for this experiment, a relatively simple model for scattering from dust clouds was developed. This model used an inverse-power-law expression for the particle-size distribution and the

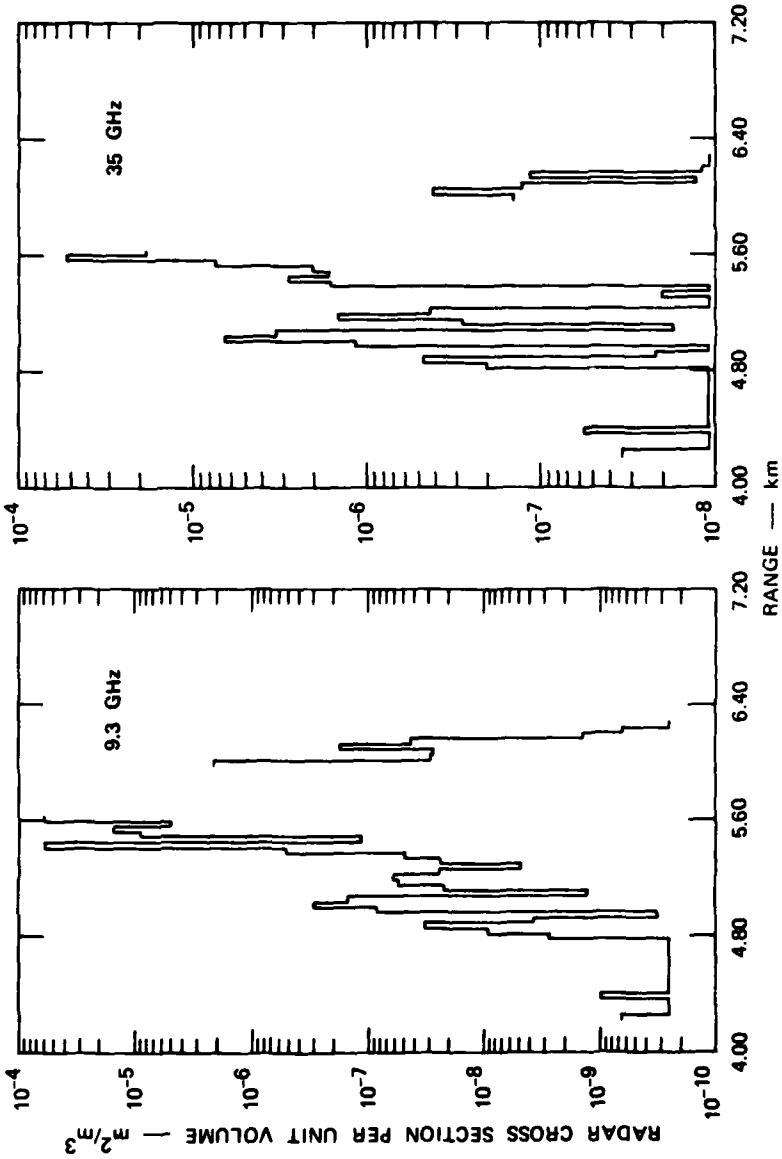

FIGURE 8 MBII-2 RADAR ECHOES AT 9.3 AND 35 GHz AT T + 16 s--AZIMUTH = 73.0°, ELEVATION = 1.4°

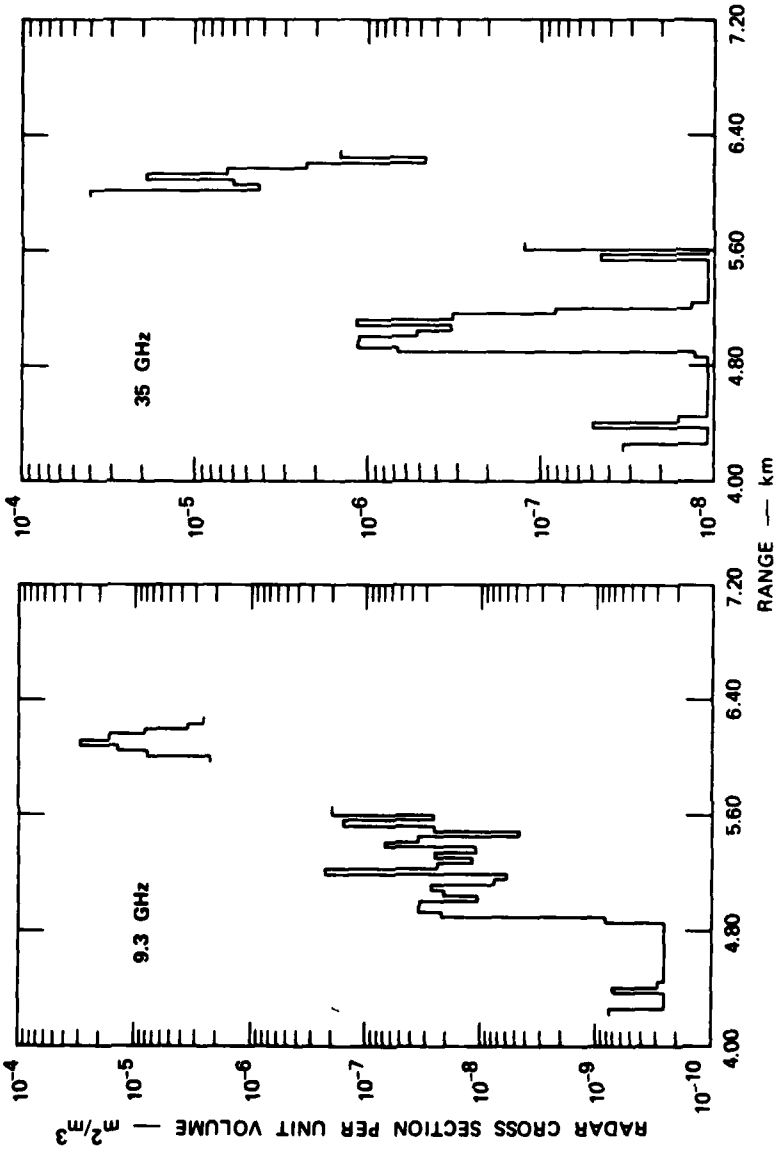

FIGURE 9 MBII-2 RADAR ECHOES AT 9.3 AND 35 GHz AT T + 42 s--AZIMUTH = 71.6°, ELEVATION = 1.8°

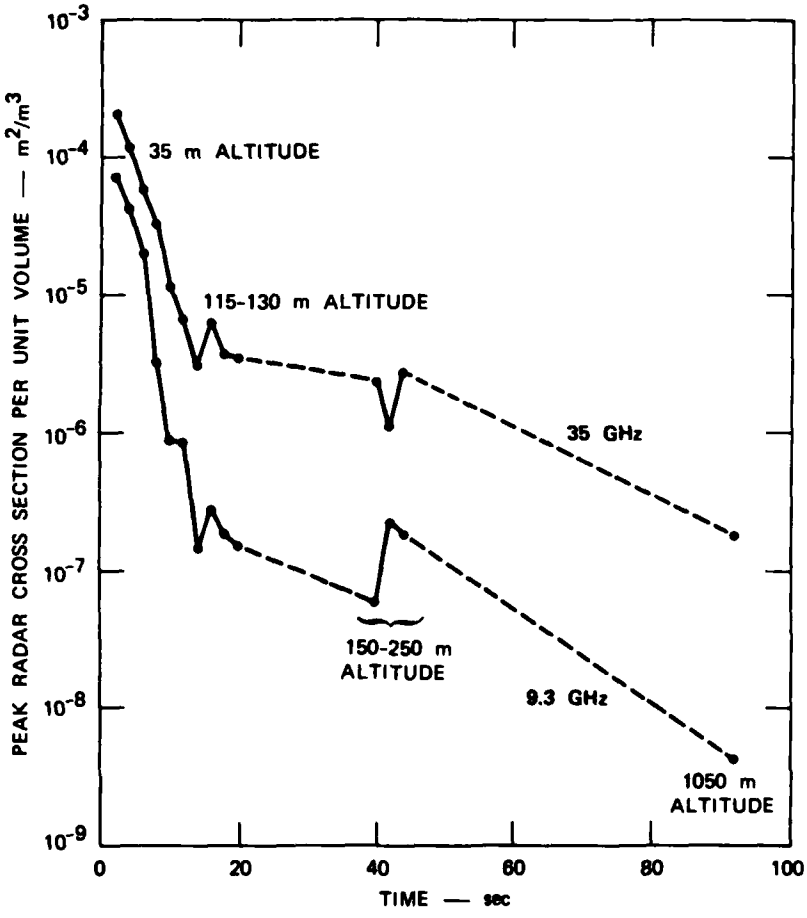

FIGURE 10 PEAK RADAR CROSS SECTION vs. TIME FOR MBII-2. The altitudes shown are those of the beam center above ground zero.

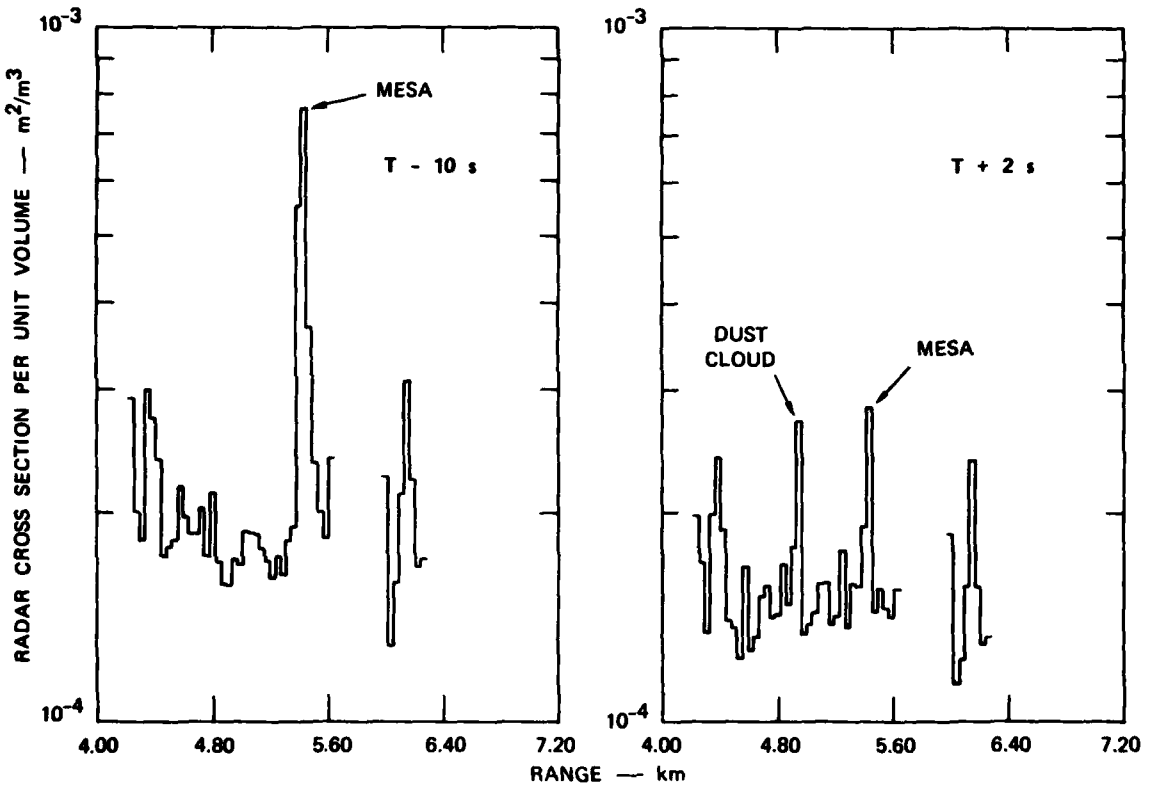

FIGURE 11 MBII-2 95-GHz RADAR ECHOES PRIOR TO AND IMMEDIATELY AFTER DETONATION

Rayleigh and geometric-optics asymptotes to describe the scattering from individual particles. Its primary purpose was to ensure that proper signal levels and dynamic range were provided. Initial dust densities were chosen by assuming that all the ejecta from a large crater was spread into a rather small volume. The power-law exponent, γ, of the particle-size distribution function was rather arbitrarily chosen, based on values commonly used. Figure 12(a) presents the results based on this model, along with some previous measurements at various times after detonation.

Figure 12(b) shows the MBII-2 results in the same format as Figure 12(a). In general, there is surprisingly good agreement, particularly with the frequency dependence and its temporal development--considering the many arbitrary aspects of the model. The inferred initial dust densities of perhaps 10 g/m^3 were several orders-of-magnitude less than expected, but the rate of decrease in inferred dust density was about that expected. The somewhat higher than expected inferred value of γ is consistent with what has been learned of the nature of the soil at the MISERS BLUFF II test site. That soil, a great deal of which has been most often described as "silt," contains a higher content of fine particles than is usually found. Again, we should caution that the results shown in Figure 12 are preliminary; because all of the conditions required by the model may not have been met, it is particularly dangerous to extract cloud-mass densities and values for γ from Figure 12 until more analysis has been completed. That analysis and complete data-reduction and evaluation efforts have just recently begun.

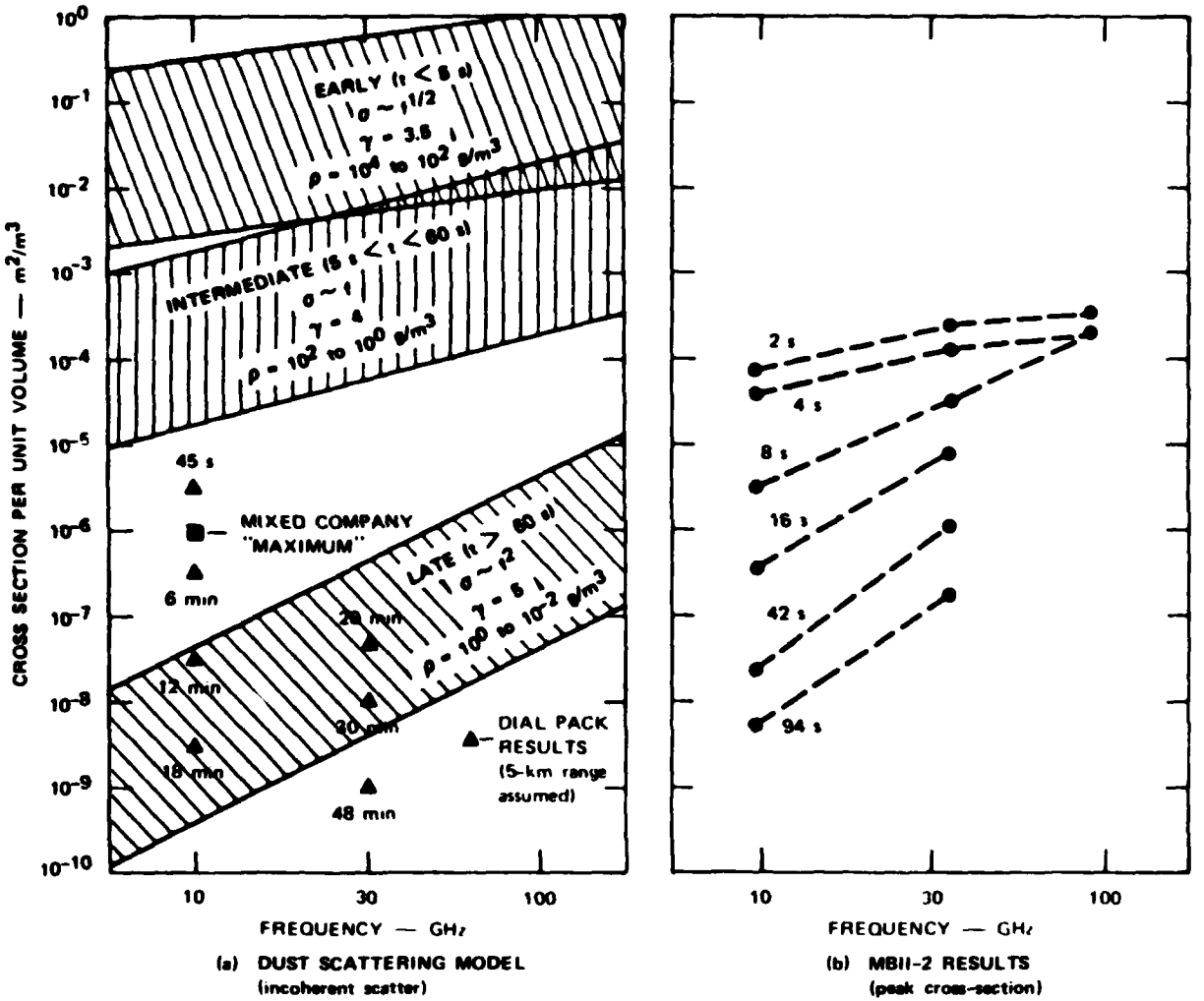

FIGURE 12 COMPARISON BETWEEN EXPERIMENT PLANNING MODEL AND MBII-2 RADAR CROSS-SECTION RESULTS

IV CONCLUSIONS

In spite of tight fielding schedules and a very hostile field environment, the two experiments described here were very successful. Nearly all of the objectives were met, and 75% to 90% of the possible data were collected. The data collected were of a very high quality and will undoubtedly increase our knowledge of the effects of dust clouds on electromagnetic propagation. The principal disappointments were the failure of the millimeter-wavelength coherent-transmission-experiment components and the low sensitivity of the 95-GHz radar.

Because of the different relative placements of the lines of sight relative to ground zero for the MBII tests, the UHF-EHF-Coherent-Transmission Experiment probed a different part of the cloud than during the DICE THROW Main Event. Furthermore, because the winds were more favorable than during DICE THROW, the MBII clouds remained in the lines-of-sight much longer. Thus the data base was greatly expanded.

The SHF/EHF-Scattering Experiment demonstrated that the dust cloud could be mapped with good resolution. We collected data from which dust-densities and size-distribution parameters and their temporal and spatial variations can be inferred. This was the first successful measurement, in our knowledge, of these parameters at early times when dust densities are very high. We also measured directly the effects of dust clouds on radar systems and their wavelength dependencies in the millimeter regime.

REFERENCES

1. J. G. Hawley and A. A. Burns, "MISERS BLUFF Electromagnetic Propagation Experiment: Preliminary Results of the Laser Radar Experiment," Topical Report for the Period 1 October 1978 to 31 March 1979, Contracts DNA001-79-C-0181 and DNA001-77-C-0269, SRI Project 8279, SRI International, Menlo Park, CA, 94025 (to be published).

2. R. S. Vickers, "Medium Frequency Propagation at MISERS BLUFF," Topical Report for the Period 15 July to 15 November 1978, Contract DNA001-77-C-0269, SRI Project 6462, SRI International, Menlo Park, CA, 94025 (to be published).

3. A. A. Burns and P. L. Crawley, "DICE THROW UHF/SHF Transmission Experiment, Volume III--Final Data Reduction and Interpretation," Topical Report for 16 November 1976 to 19 March 1979, Contract DNA001-75-C-0206, SRI Project 8279, SRI International, Menlo Park, CA, 94025 (to be published).

4. DNA, Proceedings of the DICE THROW Symposium, 21-23 June 1977, Vols. 1-3, DNA 4377P-1, -2, -3, Contract DNA001-75-C-0023, General Electric Company, TEMPO, DASIAC, Santa Barbara, CA, 93102 (July 1977).

DISTRIBUTION LIST

DEPARTMENT OF DEFENSE

Assistant Secretary of Defense
Comm., Cmd., Cont., & Intell.
ATTN: Dir. of Intelligence Systems, J. Babcock
ATTN: C3IST&CCS, M. Epstein

Assistant to the Secretary of Defense
Atomic Energy
ATTN: Executive Assistant

Command & Control Technical Center
ATTN: C-312, R. Mason
ATTN: C-650, G. Jones
3 cy ATTN: C-650, W. Heidig

Defense Advanced Rsch. Proj. Agency
ATTN: TIO

Defense Communications Agency
ATTN: Code 480, F. Dieter
ATTN: Code 101B
ATTN: Code 810, J. Barna
ATTN: Code 480
ATTN: Code 205

Defense Communications Engineer Center
ATTN: Code R123
ATTN: Code R720, J. Worthington
ATTN: Code R410, R. Craighill
ATTN: Code R410, J. McLean

Defense Intelligence Agency
ATTN: HQ-TR, J. Stewart
ATTN: DC-7D, W. Wittig
ATTN: DT-1B
ATTN: DB, A. Wise
ATTN: DB-4C, E. O'Farrell
ATTN: DT-5

Defense Nuclear Agency
ATTN: STVL
3 cy ATTN: RAAE
4 cy ATTN: TITL

Defense Technical Information Center
12 cy ATTN: DD

Field Command
Defense Nuclear Agency
ATTN: FCPR

Field Command
Defense Nuclear Agency
Livermore Division
ATTN: FCPRL

Interservice Nuclear Weapons School
ATTN: TTV

Joint Chiefs of Staff
ATTN: C3S
ATTN: C3S Evaluation Office

Joint Strat. Tgt. Planning Staff
ATTN: JLA
ATTN: JLTW-2

DEPARTMENT OF DEFENSE (Continued)

National Security Agency
ATTN: B-3, F. Leonard
ATTN: W-32, O. Bartlett
ATTN: R-52, J. Skillman

Undersecretary of Defense for Rsch. & Engrg
ATTN: Strategic & Space Systems (OS)

WWMCCS System Engineering Org.
ATTN: J. Hoff

DEPARTMENT OF THE ARMY

Assistant Chief of Staff for Automation & Comm.
Department of the Army
ATTN: DAAC-ZT, P. Kenny

Atmospheric Sciences Laboratory
U.S. Army Electronics R&D Command
ATTN: DELAS-EO, F. Niles

BMD Systems Command
Department of the Army
2 cy ATTN: BMDSC-HW

Deputy Chief of Staff for Ops. & Plans
Departmentof the Army
ATTN: DAMO-RQC

Electronics Tech. & Devices Lab.
U.S. Army Electronics R&D Command
ATTN: DELET-ER, H. Bomke

Harry Diamond Laboratories
Department of the Army
ATTN: DELHD-N-P, F. Wimenitz
ATTN: DELHD-I-TL, M. Weiner
ATTN: DELHD-N-RB, R. Williams
2 cy ATTN: DELHD-N-P

U.S. Army Comm-Elec. Engrg. Instal. Agency
ATTN: CCC-EMEO-PED, G. Lane
ATTN: CCC-CED-CCO, W. Neuendorf
ATTN: CCC-EMEO, W. Nair

U.S. Army Communications Command
ATTN: CC-OPS-W
ATTN: CC-OPS-WR, H. Wilson

U.S. Army Communications R&D Command
ATTN: DRDCO-COM-RY, W. Kesselman

U.S. Army Foreign Science & Tech. Ctr.
ATTN: DRXST-SD

U.S. Army Materiel Dev. & Readiness Command
ATTN: RCLDC, J. Bender

U.S. Army Nuclear & Chemical Agency
ATTN: Library

U.S. Army Satellite Comm. Agency
ATTN: Document Control

DEPARTMENT OF THE ARMY (Continued)

U.S. Army TRADOC Systems Analysis Activity
ATTN: ATAA-TCC, F. Payan, Jr.
ATTN: ATAA-PL
ATTN: ATAA-TDC

DEPARTMENT OF THE NAVY

Joint Cruise Missiles Project
Department of the Navy
ATTN: JCMG-707

Naval Air Development Center
ATTN: Code 6091, M. Setz

Naval Air Systems Command
ATTN: PMA 271

Naval Electronic Systems Command
ATTN: Code 3101, T. Hughes
ATTN: Code 501A
ATTN: PME 117-2013, G. Burnhart
ATTN: PME 117-20
ATTN: PME 106-13, T. Griffin
ATTN: PME 117-211, B. Kruger
ATTN: PME 106-4, S. Kearney

Naval Ocean Systems Center
ATTN: Code 5322, M. Paulson
ATTN: Code 532, J. Bickel
3 cy ATTN: Code 5324, W. Moler

Naval Intelligence Support Ctr.
ATTN: NISC-50

Naval Research Laboratory
ATTN: Code 7550, J. Davis
ATTN: Code 4700, T. Coffey
ATTN: Code 7500, B. Wald
ATTN: Code 4780, S. Ossakow

Naval Space Surveillance System
ATTN: J. Burton

Naval Surface Weapons Center
ATTN: Code F31

Naval Surface Weapons Center
ATTN: Code F-14, R. Butler

Naval Telecommunications Command
ATTN: Code 341

Office of Naval Research
ATTN: Code 421
ATTN: Code 420

Office of the Chief of Naval Operations
ATTN: OP 941D
ATTN: OP 981N
ATTN: OP 65

Strategic Systems Project Office
Department of the Navy
ATTN: NSP-43
ATTN: NSP-2141
ATTN: NSP-2722, F. Wimberly

DEPARTMENT OF THE AIR FORCE

Aerospace Defense Command
Department of the Air Force
ATTN: DC, T. Long

Air Force Geophysics Laboratory
ATTN: OPR-1, J. Ulwick
ATTN: PHI, J. Buchau
ATTN: LKB, K. Champion
ATTN: OPR, A. Stair
ATTN: PHP, J. Aarons
ATTN: PHP, J. Mullen

Air Force Weapons Laboratory
Air Force Systems Command
ATTN: SUL
ATTN: DYC

Air Force Wright Aeronautical Laboratories
ATTN: AAD, W. Hunt
ATTN: A. Johnson

Air Logistics Command
Department of the Air Force
ATTN: OO-ALC/MM, R. Blackburn

Assistant Chief of Staff
Intelligence
Department of the Air Force
ATTN: INED

Assistant Chief of Staff
Studies & Analyses
Department of the Air Force
ATTN: AF/SASC, W. Adams
ATTN: AF/SASC, G. Zank

Ballistic Missile Office
Air Force Systems Command
ATTN: MNNH
ATTN: MNNL, S. Kennedy
ATTN: MNNH, M. Baran

Deputy Chief of Staff
Operations, Plans, and Readiness
Department of the Air Force
ATTN: AFXOKS
ATTN: AFXOKCD
ATTN: AFXOKT
ATTN: AFXOXFD

Deputy Chief of Staff
Research, Development, & Acq.
Department of the Air Force
ATTN: AFRDS
ATTN: AFRDQ
ATTN: AFRDSS
ATTN: AFRDSP

Electronic Systems Division
Department of the Air Force
ATTN: DCKC, J. Clark

Electronic Systems Division
Department of the Air Force
ATTN: XRW, J. Deas

DEPARTMENT OF THE AIR FORCE (Continued)

Electronic Systems Division
Department of the Air Force
ATTN: YSM, J. Kobelski
ATTN: YSEA

Foreign Technology Division
Air Force Systems Command
ATTN: TQTD, B. Ballard
ATTN: NIIS Library
ATTN: SDEC, A. Oakes

Headquarters Space Division
Air Force Systems Command
ATTN: SKA, M. Clavin
ATTN: SKA, C. Rightmyer

Headquarters Space Division
Air Force Systems Command
ATTN: SZJ, L. Doan
ATTN: SZJ, W. Mercer

Rome Air Development Center
Air Force Systems Command
ATTN: TSLD
ATTN: OCS, V. Coyne

Rome Air Development Center
Air Force Systems Command
ATTN: EEP

Strategic Air Command
Department of the Air Force
ATTN: DCXT
ATTN: XPFS
ATTN: DCXT, T. Jorgensen
ATTN: DCX
ATTN: DCXF
ATTN: OOKSN
ATTN: NRT

DEPARTMENT OF ENERGY CONTRACTORS

EG&G, Inc.
Los Alamos Division
ATTN: D. Wright
ATTN: J. Colvin

Lawrence Livermore National Laboratory
ATTN: Technical Information Dept. Library

Los Alamos National Scientific Laboratory
ATTN: R. Taschek
ATTN: P. Keaton
ATTN: D. Westervelt

Sandia National Laboratories
ATTN: D. Dahlgren
ATTN: Space Project Div.
ATTN: 3141
ATTN: D. Thornbrough
ATTN: Org. 1250, W. Brown

Sandia National Laboratories
Livermore Laboratory
ATTN: B. Murphey
ATTN: T. Cook

OTHER GOVERNMENT AGENCIES

Central Intelligence Agency
ATTN: OSI/PSTD

Department of Commerce
National Bureau of Standards
ATTN: R. Moore

Department of Commerce
National Oceanic & Atmospheric Admin.
Environmental Research Laboratories
ATTN: R. Grubb

Institute for Telecommunications Sciences
National Telecommunications & Info. Admin.
ATTN: D. Crombie
ATTN: A. Jean
ATTN: W. Utlaut
ATTN: L. Berry

U.S. Coast Guard
Department of Transportation
ATTN: G-DOE-3/TP54, B. Romine

DEPARTMENT OF DEFENSE CONTRACTORS

Aerospace Corp.
ATTN: D. Olsen
ATTN: I. Garfunkel
ATTN: V. Josephson
ATTN: R. Slaughter
ATTN: F. Morse
ATTN: N. Stockwell
ATTN: T. Salmi
ATTN: S. Bower

University of Alaska
ATTN: Technical Library
ATTN: T. Davis
ATTN: N. Brown

Analytical Systems Engineering Corp.
ATTN: Radio Sciences

Analytical Systems Engineering Corp.
ATTN: Security

Barry Research Corp.
ATTN: J. McLaughlin

BDM Corp.
ATTN: L. Jacobs
ATTN: T. Neighbors

Berkeley Research Associates, Inc.
ATTN: J. Workman

Boeing Co.
ATTN: M/S 42-33, J. Kennedy
ATTN: G. Hall
ATTN: S. Tashird

University of California at San Diego
ATTN: H. Booker

Charles Stark Draper Lab., Inc.
ATTN: J. Gilmore
ATTN: D. Cox

DEPARTMENT OF DEFENSE CONTRACTORS (Continued)

Computer Sciences Corp.
ATTN: H. Blank

COMSAT Labs.
ATTN: G. Hyde
ATTN: R. Taur

Cornell University
ATTN: D. Farley, Jr.

Electrospace Systems, Inc.
ATTN: H. Logston

ESL, Inc.
ATTN: J. Marshall

Ford Aerospace & Communications Corp.
ATTN: J. Mattingley

General Electric Co.
ATTN: M. Bortner
ATTN: A. Harcar

General Electric Co.
ATTN: C. Zierdt
ATTN: A. Steinmayer

General Electric Co.
ATTN: F. Reibert

General Electric Company—TEMPO
ATTN: M. Stanton
ATTN: D. Chandler
ATTN: T. Stevens
ATTN: DASIAC
ATTN: W. Knapp

General Electric Tech. Services Co., Inc.
ATTN: G. Millman

General Research Corp.
ATTN: J. Ise, Jr.
ATTN: J. Garbarino

Georgia Institute of Technology
ATTN: Eng. Expt. Sta., E. Martin

GTE Sylvania, Inc.
ATTN: M. Cross

HSS, Inc.
ATTN: D. Hansen

IBM Corp.
ATTN: F. Ricci

University of Illinois
ATTN: K. Yeh

Institute for Defense Analyses
ATTN: E. Bauer
ATTN: H. Wolfhard
ATTN: J. Aein
ATTN: J. Bengston

International Tel. & Telegraph Corp.
ATTN: Technical Library
ATTN: G. Wetmore

DEPARTMENT OF DEFENSE CONTRACTORS (Continued)

JAYCOR
ATTN: S. Goldman

JAYCOR
ATTN: D. Carlos

Johns Hopkins University
ATTN: T. Potemra
ATTN: P. Komiske
ATTN: Document Librarian
ATTN: T. Evans
ATTN: J. Newland
ATTN: B. Wise

Kaman Sciences Corp.
ATTN: T. Meagher

Linkabit Corp.
ATTN: I. Jacobs

Litton Systems, Inc.
ATTN: R. Grasty

Lockheed Missiles & Space Co., Inc.
ATTN: R. Johnson
ATTN: M. Walt
ATTN: W. Imhof

Lockheed Missiles & Space Co., Inc.
ATTN: D. Churchill
ATTN: Dept. 60-12

M.I.T. Lincoln Lab.
ATTN: L. Loughlin
ATTN: D. Towle

McDonnell Douglas Corp.
ATTN: G. Mroz
ATTN: J. Moule
ATTN: N. Harris
ATTN: W. Olson

Meteor Communications Consultants
ATTN: R. Leader

Mission Research Corp.
ATTN: D. Sowle
ATTN: R. Hendrick
ATTN: F. Fajen
ATTN: S. Gutsche
ATTN: R. Bogusch

Mitre Corp.
ATTN: A. Kymmel
ATTN: G. Harding
ATTN: B. Adams
ATTN: C. Callahan

Mitre Corp.
ATTN: M. Horrocks
ATTN: W. Foster
ATTN: W. Hall

Pacific-Sierra Research Corp.
ATTN: E. Field, Jr.

Pennsylvania State University
ATTN: Ionospheric Research Lab.

DEPARTMENT OF DEFENSE CONTRACTORS (Continued)

PhotoMetrics, Inc.
ATTN: I. Kofsky

Physical Dynamics, Inc.
ATTN: E. Fremouw

R & D Associates
ATTN: W. Karzas
ATTN: M. Gantsweg
ATTN: R. Turco
ATTN: C. Greifinger
ATTN: W. Wright, Jr.
ATTN: B. Gabbard
ATTN: R. Lelevier
ATTN: C. MacDonald
ATTN: H. Ory
ATTN: F. Gilmore
ATTN: P. Haas

R & D Associates
ATTN: B. Yoon
ATTN: L. Delaney

Rand Corp.
ATTN: E. Bedrozian
ATTN: C. Crain

Riverside Research Institute
ATTN: V. Trapani

Rockwell International Corp.
ATTN: J. Kristof

Santa Fe Corp.
ATTN: E. Ortlieb

Science Applications, Inc.
ATTN: J. McDougall
ATTN: D. Hamlin
ATTN: L. Linson
ATTN: C. Smith
ATTN: D. Sachs
ATTN: E. Straker

DEPARTMENT OF DEFENSE CONTRACTORS (Continued)

Science Applications, Inc.
ATTN: D. Divis

Science Applications, Inc.
ATTN: SZ

SRI International
ATTN: C. Rino
ATTN: D. Neilson
ATTN: R. Livingston
ATTN: M. Baron
ATTN: R. Leadabrand
ATTN: W. Chesnut
ATTN: W. Jaye
ATTN: G. Smith
ATTN: A. Burns
ATTN: G. Price

Teledyne Brown Engineering
ATTN: R. Deliberis

TRI-COM, Inc.
ATTN: D. Murray

Utah State University
ATTN: L. Jensen
ATTN: K. Baker

Visidyne, Inc.
ATTN: J. Carpenter

TRW Defense & Space Sys, Group
ATTN: D. Dee
ATTN: R. Plebuch
ATTN: S. Altschuler

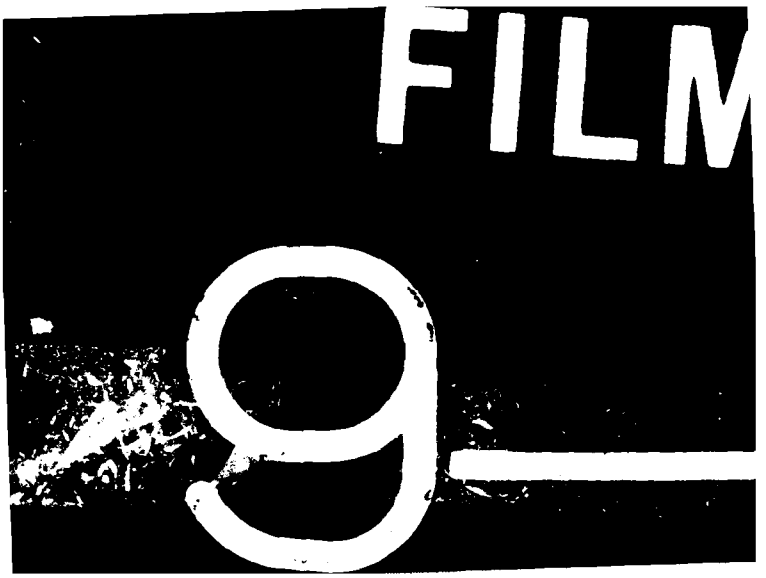
FILM
9

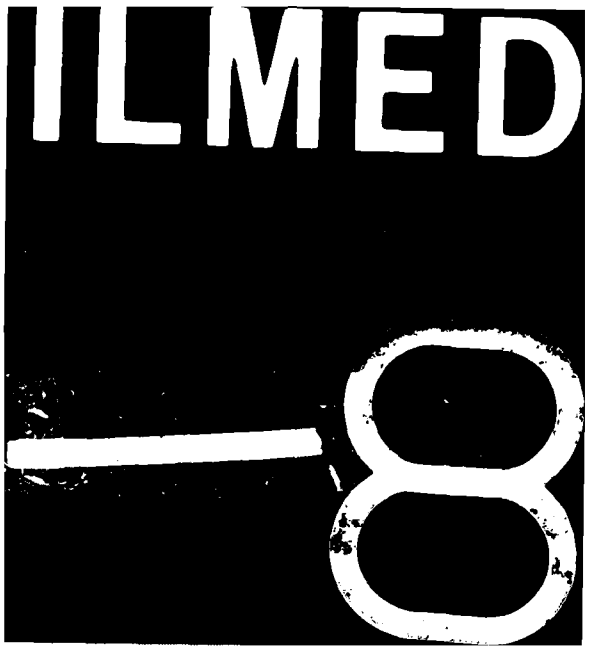
ILMED